Bifurcations and the Gauge Structure of the Standard Model

Ervin Goldfain

Ronin Institute, Montclair, New Jersey 07043, USA

E-mail ervin.goldfain@ronininstitute.org

Abstract

As of today, the reason for the unique composition of the Standard Model (SM) gauge group $SU(3)_c \times SU(2)_L \times U(1)$ remains elusive. Taking complex-scalar field theory as baseline model, we argue here that the SM group unfolds sequentially from bifurcations driven by the Renormalization scale. Numerical estimates are found to be reasonably consistent with experimental data.

Key words: Bifurcations, Feigenbaum route to chaos, complex-scalar field theory, gauge symmetries, Standard Model, electroweak model.

1. Introduction

By construction, SM is a non-Abelian gauge field theory built from the symmetry group $SU(3)_c \times SU(2)_L \times U(1)$. This group has 8+3+1=12

generators with a non-trivial commutator algebra and describes the electroweak (EW) coupling of leptons and quarks, as well as the strong interaction of quarks and gluons. [1-2]. SM contains an octet of gluons associated with the SU (3) color generators, and a quartet of EW gauge bosons W^+, W^-, Z^0, and γ. Gluons and the photon γ are massless because the symmetry induced by the other three generators is spontaneously broken. *Spontaneous symmetry breaking* (SSB) takes place in the EW sector and is characterized by the following attributes [2]

a) It occurs when there is a family of degenerate vacua transforming onto one another under the action of the gauge group. The symmetry is spontaneously broken as the system eventually settles in one of its vacua.

b) SSB is enabled in Quantum Field Theory because the latter has an unbounded number of degrees of freedom prone to undergo vacuum tunneling.

c) Since gauge symmetry is local and spontaneously broken, the associated Goldstone bosons morph into the third polarization of the W^+, W^-, Z^0 bosons, rendering them massive in the process.

The goal of this work is to offer an alternative scenario to the standard SSB interpretation, approximately matching its content and predictions. Our scenario stems from the theory of bifurcations applied to classical scalar field theory. We find that, unlike the SSB paradigm, massive electroweak bosons do not arise from the absorption of Goldstone bosons, but from the *geometry of the bifurcation process*, along with *boson condensation* induced by the minimal fractality of spacetime above the EW scale. A prerequisite of this scenario is the mechanism of *decoherence*, which acts near the EW scale and drives the transition from quantum to classical behavior [3]. Appealing to the complex-scalar field theory as baseline model, we speculate that the SM group unfolds sequentially from the flow of the Renormalization scale. Numerical estimates are found to be reasonably consistent with experimental data.

The paper is partitioned in the following way: next section elaborates on the relationship between complex-scalar field theory and the global $U(1)$ symmetry; the cubic map representation of field dynamics is derived in section three, while the bifurcation analysis of the map is developed in the next couple of sections; Section six displays a comparison between numerical estimates and experimental data; Concluding remarks are detailed in the last section.

The reader is urged to keep in mind that this work is strictly introductory in nature. It is a sequel to our previous contributions and requires independent validation, rebuttal, or further refinements.

2. Free complex-scalar fields and the *U (1)* symmetry

Consider a classical complex-scalar field described by the pair of independent components

$$\Phi = \frac{1}{\sqrt{2}}(\Phi_1 + i\,\Phi_2) \tag{1a}$$

$$\Phi^* = \frac{1}{\sqrt{2}}(\Phi_1 - i\,\Phi_2) \tag{1b}$$

One associates to (1) the massive Lagrangian

$$L = \partial_\mu \Phi \, \partial^\mu \Phi^* - m^2 \Phi^* \Phi \tag{2}$$

which is invariant under the global gauge transformation

$$\Phi \to \exp(-i\eta)\Phi \tag{3a}$$

$$\Phi^* \to \exp(i\eta)\,\Phi^* \tag{3b}$$

where η is a real constant. The conserved current induced by (3) is given by

$$J^\nu = i(\Phi^* \partial^\nu \Phi - \Phi \, \partial^\nu \Phi^*) \tag{4a}$$

with the vanishing four-divergence

$$\partial_\nu J^\nu = 0 \tag{4b}$$

and conserved charge

$$Q = \int J^0 d^3x = i \int (\Phi^* \frac{\partial \Phi}{\partial t} - \Phi \frac{\partial \Phi^*}{\partial t}) \, d^3x \,; \quad \frac{dQ}{dt} = 0 \tag{5}$$

Since $\exp(i\eta)$ represents a unitary "matrix" in one dimension, that is,

$$\exp(i\eta)[\exp(i\eta)]^+ = 1 \tag{6a}$$

the gauge transformation (3) amounts to a rotation in field space

$$\Phi_1^r = \Phi_1 \cos\eta + \Phi_2 \sin\eta \tag{6b}$$

$$\Phi_2^r = -\Phi_1 \sin\eta + \Phi_2 \cos\eta \tag{6c}$$

which is representative for the symmetry group $U(1)$.

It follows from this analysis that gauge invariant complex-scalar field theory inherently carries a *global* $U(1)$ charge. Moreover, demanding invariance of (2) under a *local* gauge transformation, gives rise to the electromagnetic field and its conserved charge Q [4]. The emergence of $U(1)$ symmetry in complex-scalar field theory will be revisited in section 5.

3. Self-interacting scalar fields as cubic maps

The goal of this section is to explore the dynamics of self-interacting field theory in connection to the flow of the Higgs scalar with the energy scale. To this end, we start from the Lagrangian

$$L_c = \partial^\mu \Phi \, \partial_\mu \Phi^* - V(\Phi\Phi^*) \tag{7}$$

in which the potential function assumes the form [2, 13]

$$V(\varphi) = \lambda(|\varphi|^2 - \frac{1}{2}\mathrm{v}^2)^2 \tag{8}$$

and where

$$|\varphi|^2 = \Phi\Phi^* \tag{9}$$

For simplicity, we omit below the modulus notation and write

$$|\varphi| \to \varphi \tag{10}$$

The flow of (10) with the normalized energy scale μ/μ_0 is given by

$$\dot{\varphi} = \mu\frac{d\varphi}{d\mu} = \frac{d\varphi}{d[\log(\mu/\mu_0)]} = \frac{d\varphi}{d\tau} \tag{11}$$

in which μ_0 is an arbitrary reference scale. One obtains

$$\dot{\varphi} = -\frac{\partial V(\varphi)}{\partial\varphi} = 2\lambda\varphi(\mathrm{v}^2 - 2\varphi^2) \tag{12}$$

(12) may be rendered in a more familiar form through the substitution

$$y = \frac{\sqrt{2}}{\mathrm{v}}\varphi \tag{13}$$

Since φ and v have mass dimension $[\varphi]=[\mathrm{v}]=M$, dimensional consistency requires passing to the normalized control parameter

$$m=\frac{2\lambda \mathrm{v}^2}{m_0^2} \tag{14a}$$

where m_0 is an arbitrary reference mass. (14a) runs with the energy scale as in

$$m=m(\tau);\ \lambda=\lambda(\tau);\ \ m_0=m_0(\tau) \tag{14b}$$

One finds that (12) reduces to the equation

$$\dot{y}=my(1-y^2) \tag{15}$$

By assumption A3) below, the map analog of (15) around the origin $y=0$ may be presented as (Appendix A)

$$\boxed{y_{n+1}=f(m,y_n)=my_n(1-y_n^2)} \tag{16}$$

where the ranges of the control parameter and the y variable are set to, respectively,

$$0 \le m \le 3; \quad -1 \le y \le 1 \tag{17}$$

4. Working assumptions

A1) The flow (16) evolves in non-equilibrium conditions and (at least in principle) is incompatible with the perturbative Renormalization Group, where quantum fluctuations are present and the flow equations asymptotically settle on a finite number of stationary attractors [8, 11, 14, 17-18].

A2) Non-equilibrium regime near or above the EW scale implies *statistical behavior* in the classical sense, as well as the onset of *decoherence* triggered by chaotic mixing and diffusion [3]. Obviously, a more realistic setup must account for effects that are absent from (12) and (16), such as a) random perturbations with short or long correlations or b), the *self-interacting* nature of electroweak bosons.

A3) Following the ideas of [6-8, 12], *topological condensation* reflects the confining behavior of spacetime endowed with minimal fractality. This condensation mechanism is similar (but not identical) to the Anderson

localization of quantum waves in random potentials. It leads to the formation of weakly coupled clusters of scalar or vector bosons. A corollary of this assumption is that the *transfinite and discrete nature* of spacetime endowed with minimal fractality motivates replacing the differential equation (15) with the map (16).

A4) The bifurcation process is associated with broken symmetries defining critical phenomena [14-16, 18]. In our context, symmetry breaking is a combined outcome of nonlinearity and fast bifurcations, commensurate in duration with the EW scale [10]. We posit below that the upper bifurcation branches contain exclusively boson condensates, whereas lower branches nearly free boson states.

A5) For simplicity, we assume that $\lambda(\tau)$ runs much faster than $m_0(\tau)$, that is, $\dot{\lambda} >> \dot{m}_0$. While this assumption is unwarranted in real life, it serves here as a convenient approximation.

5. Bifurcation analysis

The fixed points of (16) are determined by

$$y_n^* = f(m, y_n^*) \tag{18}$$

leading to a trivial and a pair of symmetric solutions, i.e.

$$y^* \Rightarrow 0, \pm\sqrt{1-\frac{1}{m}} \tag{19}$$

The fixed point $y^* = 0$ is attracting (stable) for $m < 1$ and repelling (unstable) for $m > 1$. It can be also shown that the fixed points $y^* = \pm\sqrt{1-\frac{1}{m}}$ are both stable for $1 < m < 2$ and unstable for $2 < m < 3$ [5]. The bifurcation diagram of (16) (pictured below) displays the progressive generation of its critical points $y^*(m)$ under the flow of $m = m(\tau)$. In what follows, bifurcation vertices are indexed in natural progression V_i, $(i = 1, 2, ...)$. The lower and upper branches are denoted using different subscripts and superscripts, respectively, as in V_i^j, $j = 1, 2, ...$

As the diagram indicates, for $0 < m < 1$, the $y = 0$ branch contains the $U(1)$ symmetry and its conserved charge Q. The first bifurcation occurs at [5]

$$m(V_1) = 1; \;\; y^*(V_1) = 0 \tag{20a}$$

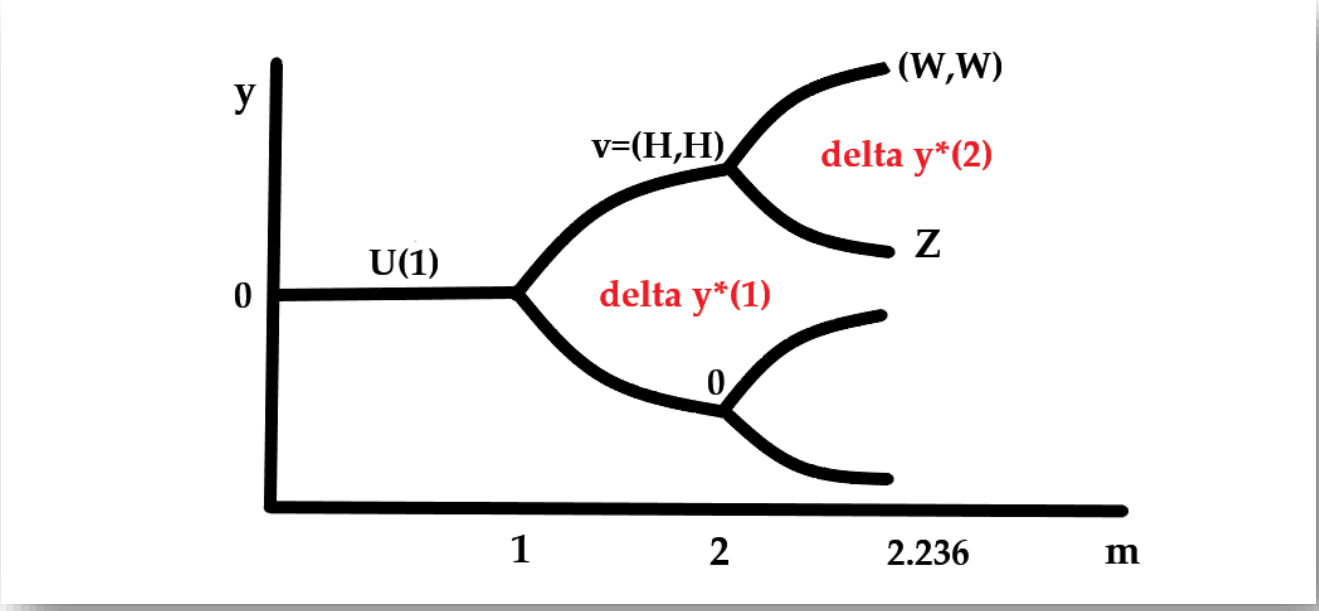

Fig. 1: Bifurcation diagram of the cubic map (16)

It is seen that (20a) recovers the SM Higgs mass in the form [1-2]

$$\boxed{m_0^2 = m_H^2 = 2\lambda \mathrm{v}^2} \tag{20b}$$

The second bifurcation occurs at

$$m(V_2) = 2\,;\quad y^*(V_2^1) = \sqrt{1-\frac{1}{2}}\,;\quad y^*(V_2^2) = -\sqrt{1-\frac{1}{2}} \tag{21}$$

The separation between the two branches amounts to

$$\Delta y^*(1) = y^*(V_2^1) - y^*(V_2^2) = \sqrt{2} \tag{22}$$

By (13), the critical point at $m(V_2) = 2$ expressed in terms of the scalar field is given by

$$\Delta\varphi^*(1) = \mathrm{v} \tag{23a}$$

Relation (23a) is consistent with the standard SSB mechanism, whereby symmetry breaking implies picking a preferential direction in $SU(2)$ space corresponding to the Higgs vacuum [1-2, 7]. By A3) and A4), the vertex V_2^1 contains a scalar condensate that we choose to identify with a *weakly coupled Higgs doublet*. In symbolic form we write

$$\mathrm{v} \Rightarrow (H, H) \tag{23b}$$

The next bifurcation develops at [5]

$$m(V_3) = 2.236 \tag{24}$$

and generates a set of four critical points as in

$$y^*(V_3^1) = \sqrt{\frac{1}{2} + \sqrt{\frac{1}{4} - \frac{1}{m^2}}}\,; \quad y^*(V_3^2) = \sqrt{\frac{1}{2} - \sqrt{\frac{1}{4} - \frac{1}{m^2}}} \tag{25a}$$

$$y^*(V_3^3) = -y^*(V_3^2)\,; \quad y^*(V_3^4) = -y^*(V_3^1) \tag{25b}$$

Using again A3) and A4), we choose to identify the condensate at V_3^1 with the pair of vector bosons (W^+, W^-). The separation between the two branches at this vertex is

$$\Delta y^*(2) = y^*(V_3^1) - y^*(V_3^2) = 0.325 \tag{27}$$

The ratio between (27) and (22) amounts to

$$\chi = \frac{\Delta y^*(2)}{\Delta y^*(1)} = 0.22981 \tag{28}$$

which, by (23a), yields

$$\frac{\Delta \varphi^*(2)}{\mathrm{v}} = \chi \tag{29}$$

Summarizing the results of this section and on account of A3) and A4), we are led to suggest the following mass relationships

$$\mathrm{v} \approx 2m_H \tag{30a}$$

$$\mathrm{v} \approx 2m_W + m_Z \tag{30b}$$

$$\Delta\varphi^*(2) = \chi \mathrm{v} \approx 2m_W - m_Z \tag{30c}$$

6. Estimates versus existing data

The aim of this section is to compare (30a) - (30c) against existing theoretical and experimental data. To this end, we choose to define the following set of *mass errors* (E) and *normalized mass errors* (e) as in

$$E_H = \mathrm{v} - 2m_H \tag{31a}$$

$$E_{WZ} = \mathrm{v} - (2m_W + m_Z) \tag{31b}$$

$$E_\Delta = (2m_W - m_Z) - \chi \mathrm{v} \tag{31c}$$

$$e_i = \frac{E_i}{\mathrm{v}_{SM}}; \quad i = \{H, WZ, \Delta\} \tag{31d}$$

(31d) is built under the assumption that the SM vacuum (v_{SM}) sets the *natural scale* of SSB in the EW sector. Results are displayed below based on the following SM input parameters (in GeV):

$$\mathrm{v}_{SM} = 246; \quad m_H = 125.35$$

$$m_W = 80.385; \quad m_Z = 91.1876$$

e_H (%)	1.91
e_{WZ} (%)	2.42
e_Δ (%)	5.28

Tab. 1: Mass errors normalized to the SM vacuum

An error reduction approach applied to the entries of Tab. 1 is detailed in Appendix C.

7. Conclusions and follow-up challenges

We examined an alternative scenario to the standard Higgs paradigm of SSB, approximately matching its content and predictions. Working in the context of classical complex-scalar field theory, an alternative mass-generating mechanism was proposed, driven by bifurcations and boson condensation on spacetime having minimal fractality.

Despite their apparent similarity, the standard SSB mechanism and the proposed bifurcation model (BM) differ in many respects. In particular,

a) Per section 1, the analysis is carried out in an entirely *classical framework.*

b) Unlike the SSB mechanism, vector bosons *do not preexist* the Higgs field, but are *generated from* the dynamic instability of its vacuum.

c) As conjectured in [23], BM can account for the hierarchy of quark and lepton mass ratios, as well as the hierarchy of mixing angles, via the Feigenbaum route to chaos in unimodal maps. It can also account for the triplication of fermion families and the chiral nature of the fermionic sector [23].

Notwithstanding its appeal, a rigorous completion of the BM requires further analysis and clarifications. Here is a partial list of open challenges:

1) How does BM accommodate the Goldstone bosons created by global symmetry breaking? Are they associated with the unstable branch $y = 0$ at V_1 and $1 < m < 2$, which is unobservable in real life?

2) Is there an underlying connection between BM and the phase diagram of lattice gauge theories [14, 19-20]? Do the Coulomb, Higgs, and confined phases match their respective vertices of BM?

3) How is the gluon octet generated via bifurcations at V_j; $j > 2$? Do gluons still arise as weakly coupled condensates or do they form a confined strongly coupled phase, fundamentally distinct from the EW phase? More generally, as anticipated in [23], how do fermion vertices develop in BM? Moreover, how do particle interaction channels relate to transformations within the bifurcation diagram?

4) How does one reconcile the scalar nature of the Higgs boson with the vector nature of EW bosons [7, 12]?

5) Can the chirality of EW bosons be linked to the asymmetric properties of a spacetime endowed with minimal fractality [24]?

The behavior of (16) was analyzed under the hypothesis that it represents a reasonable, coarse-grained description of (15) [21]. As alluded to in assumption A2), a more comprehensive treatment may consider placing the

Higgs dynamics in two or more dimensions, including the effect of self-interaction and accounting for the *non-perturbative run of particle masses with the Renormalization scale* (Appendix B).

It is known that unitary symmetry groups reflect rotations in field space leaving the Lagrangian invariant. In a broader perspective, one can conceivably argue that rotations preserving the Lagrangian are reducible to ***self-similarity transformations*** [22]**.** If this interpretation stands, the bifurcation cascade initiated at V_1 replicates the action of symmetry groups $SU(n)$ with n in ascending order.

It is also instructive to note that, at least in principle, supplementing (31) with additional constraints imposed by the "sum-of-squares" relationship [8-9, 13] enables the derivation of EW boson masses in *closed-form*. The "sum-of-squares" relationship constrains the overall number of SM flavors [13].

APPENDIX A: Derivation of the cubic map

The map representation of the differential equation

$$\dot{y} = my(1-y^2) \tag{32}$$

follows from its discretization, which gives the approximation

$$y_{n+1} = y_n + \tau_0 m y_n (1 - y_n^2) \tag{33}$$

where τ_0 is the "time-like" step associated with (11) [21]. Carrying out the substitution

$$\tau_0 m = \frac{2\tau_0 \lambda \mathrm{v}^2}{m_0^2} = \frac{2\lambda' \mathrm{v}^2}{m_0^2} \tag{34}$$

recovers the cubic map (16) under the following assumed constraints

$$\left| \frac{2\lambda' \mathrm{v}^2}{m_0^2} (1 - y_n^2) \right| >> 1; \quad |y_n| << 1 \tag{35}$$

By (11) and assumption A1), the "time-like" step τ_0 amounts to setting a finite cutoff on the scale μ/μ_0, written as $\tau_0 = \Delta\mu/\mu_0$. If m_0 is chosen to be on the order of magnitude of the SM Higgs mass ($m_0 \approx m_H$), by (11) and (30a) the condition (35) yields

$$\frac{\Delta\mu}{\mu_0} >> \exp\left(\frac{1}{8\lambda}\right) \tag{36}$$

It is apparent that (36) complies with the choice $\mu_0 = O(\Lambda_{IR})$, with $\Lambda_{IR} << \mathrm{v}$ a deep infrared (IR) scale far lower than the EW vacuum. Moreover, since v fixes the SSB scale, the case can be made that setting $\Delta\mu << \mathrm{v}$ provides a small enough step suitable for the numerical evaluation of (16).

In summary, the validity of (16) relies on the following couple of constraints

$$\mu_0 = \Lambda_{IR} << \Delta\mu << \mathrm{v} \tag{37}$$

It is instructive to note that there is an alternative method of passing from (15) to (16) that circumvents the constraints (35)-(37). Performing the change of variables [25]

$$r = 1 + m\tau_0 \tag{38a}$$

$$z_n = k y_n \tag{38b}$$

$$k^2 = \frac{m\tau_0}{r} \tag{38c}$$

turns (33) into

$$z_{n+1} = r z_n (1 - z_n^2) \tag{39}$$

which is formally identical to (16). However, in this case, the pitchfork bifurcation at $r=1$ corresponds to $m\to 0, \lambda\to 0$, which reflects a *different physical setting* than the one described in this work.

APPENDIX B: Accounting for memory effects

An interesting setting arises if (15) is allowed to become time-dependent and include memory effects. In this case, (15) gets replaced with the *fractional differential equation* [26]

$$D^{\alpha}y = my(1-y^2) \tag{B1}$$

where $\alpha(\tau)$ is the index of fractional differentiation. Because we are considering a spacetime support endowed with minimal fractality, the natural choice for the index is

$$\alpha(\tau) = 1-\varepsilon(\tau) \tag{B2}$$

in which [8]

$$\varepsilon(\tau) = \frac{m^2(\tau)}{\Lambda_{UV}^2} << 1 \tag{B3}$$

with Λ_{UV} a large ultraviolet scale. Replacing (B1) with its approximation in the regime of low-level fractionality turns (15) into [26]

$$\dot{y} \approx my(1-y^2)+\Phi[\varepsilon(\tau)] \tag{B4}$$

As a result, the map (16) becomes dependent on (B3), which means that *mass generation at each bifurcation vertex is now inherently coupled with mass generation at all other vertices*. This counterintuitive result reflects nonlocal mixing and the violation of the clustering theorem, typical for the onset of chaos and non-integrability [27].

APPENDIX C: Enhancing mass estimates through error analysis

Allowing (15) and (16) to be impacted by memory effects also implies that numerical uncertainties *carry over* from one bifurcation vertex to the next. The object of this Appendix is to show that a closer match between mass predictions and experimental data is obtained upon accounting for error propagation among neighboring vertices. To this end we assume that a) the estimation error at $V_i, (i=1, 2, 3, ...)$ transfers to the next vertex V_{i+1} and b), the

errors at V_2 (denoted δV_2) and V_3 (denoted δV_3) are subtracted out from their respective entries of Tab. 1.

Tabulating the mass errors derived from (31) gives the entries of Tab.2 below,

E_H	4.70
E_{WZ}	5.96
E_Δ	13.05

Tab 2: Mass errors (GeV) from (31)

Vertex errors are expected to add in quadrature and therefore,

$$E_i \propto \sqrt{\sum_j (\delta V_i^j)^2} \tag{C1}$$

which means that,

$$E_1 \propto \sqrt{(\delta V_1)^2} = \delta V_1 \tag{C2}$$

$$E_2 \propto \sqrt{\sum_1^2 (\delta V_2^j)^2} \tag{C3}$$

$$E_3 \propto \sqrt{\sum_1^4 (\delta V_2^j)^2} \tag{C4}$$

If errors incurred within the same vertex are conjectured to be of equal magnitude ($\delta V_i^j = \delta V_i^{j+1}, \forall j$), (C1) - (C4) imply

$$\delta V_2 = E_1, \quad \delta V_3 = E_2 \tag{C5}$$

and lead to

$$E_2 = \sqrt{2} E_1, \quad E_3 = 2E_2 \tag{C6}$$

The corrected mass errors computed using (C6) are displayed in the second and third row of Tab.3,

$E_{c,H}$	$E_H = 4.70$
$E_{c,WZ}$	$\sqrt{2}E_{c,H} = 6.65$
$E_{c,\Delta}$	$2E_{c,WZ} = 13.30$

Tab.3: Corrected mass errors (GeV) from (C6)

Repeating the computation of normalized mass errors (31d) using the prescription

$$e_{c,i} = \frac{E_{c,i} - E_i}{\mathrm{v}_{SM}}; \quad i = \{WZ, \Delta\} \tag{C7}$$

yields the results displayed in Tab.4.

$e_{c,H}$ (%)	1.91
$e_{c,WZ}$ (%)	0.28
$e_{c,\Delta}$(%)	0.10

Tab. 4: Corrected mass errors normalized to the SM vacuum

References

1. https://link.springer.com/content/pdf/10.1007%2F978-3-319-51920-3.pdf

2. Maggiore, M. A Modern Introduction to Quantum Field Theory, Oxford Univ. Press, 2006.

3. https://arxiv.org/pdf/1810.02319.pdf

4. Ryder, L. H., Quantum Field Theory, Cambridge Univ. Press, 1989.

5. Available at the following site

https://www.researchgate.net/publication/303819069_VARIOUS_BIFURCATIONS_IN_A_CUBIC_MAP

6. https://arxiv.org/pdf/2003.07188.pdf

7. Available at the following site

https://www.researchgate.net/publication/346688804_Higgs_Mass_from_Topological_Condensation_of_Vector_Bosons

8. Available at the following site

https://www.researchgate.net/publication/278849474_Introduction_to_Fractional_Field_Theory_consolidated_version

9. Available at the following site:

https://www.researchgate.net/publication/343426122_Derivation_of_the_Sum-of-Squares_Relationship

10. Available at the following site

https://www.researchgate.net/publication/253209054_Probability_Symmetry_Broken_upon_Rapid_Period-Doubling_Bifurcation

11. http://www.ejtp.com/articles/ejtpv7i24p219.pdf

12. Goldfain, E. "Fractal Spacetime as Underlying Structure of the Standard Model", Quantum Matter, 3 (3), 2013, pp. 256-263.

13. https://arxiv.org/pdf/1305.4208.pdf

14. Bruce, A. and Wallace, D. "Critical point phenomena: universal physics at large length scales", in *The New Physics*, Cambridge Univ. Press, 1992, pp. 236-267.

15. Grosse H., Models in Statistical Physics and Quantum Field Theory, Springer-Verlag, 1988.

16. Lesne A. and Laguës M., Scale Invariance: from Phase Transitions to Turbulence, Springer-Verlag, 2012.

17. https://arxiv.org/pdf/hep-th/0304178.pdf

18. https://arxiv.org/pdf/cond-mat/0611353.pdf

19. https://arxiv.org/pdf/1211.2843.pdf

20. https://eduardo.physics.illinois.edu/phys583/ch18.pdf

21. Collet P. and Eckman J. P., Iterated maps on the interval as dynamical systems, Birkhäuser, Boston, 1980.

22. Available at the following site

https://www.researchgate.net/publication/342876637

23. Available at the following sites

https://www.sciencedirect.com/science/article/abs/pii/037843719090008G

https://www.researchgate.net/publication/343686626_Three_Generations_and_Fermion_Chirality_from_Universal_Bifurcations

https://www.researchgate.net/publication/343863324_Addendum_to_A_Bifurcation_Model_of_the_Quantum_Field

https://www.researchgate.net/publication/344036923_Mass_Hierarchy_and_Mixing_Matrices_from_Universal_Bifurcations

24. Available at the following site

https://www.sciencedirect.com/science/article/abs/pii/S1007570406001183

25. http://www.maths.qmul.ac.uk/~sb/cf_chapter3.pdf

26. https://arxiv.org/abs/physics/0511138

27. https://www.researchgate.net/publication/349476440